RECyT
Year 26 / Nº 42 / 2024 / 65–71
DOI: https://doi.org/10.36995/j.recyt.2024.42.007

Characterization of activated carbon produced from industrial waste of yerba mate by chemical activation with $ZnCl_2$

Caracterización de carbón activado producido a partir de residuos industriales de yerba mate mediante activación química con $ZnCl_2$

Sergio Alejandro Surkan[1, 2, *]; Claudia Marcela Mendez[1]; Marcos Gabriel Maiocchi[3]

1- School of Exact, Chemical and Natural Sciences, National University of Misiones (FCEQyN). Posadas, Misiones, Argentina.
2- National Institute of Yerba Mate. Argentina.
3- School of Exact and Natural Sciences and Surveying, National University of the Northeast. Argentina.
* E-mail: sasurkan@gmail.com

Received: 30/11/2023; Accepted: 05/11/2024

Abstract

In this study, activated carbons (ACs) were prepared by chemical activation with $ZnCl_2$ of yerba mate (YM) branches in a ratio of 1:1 mass of carbon vs. mass of activating agent, performing the pyrolysis at 550, 650, and 750°C in a stream of nitrogen for 60 and 120 minutes. The resulting AC were characterized by various techniques, such as Brunauer-Emmett-Teller (BET) analysis, Fourier transform infrared spectroscopy (FTIR), scanning electron microscopy (SEM), and X-ray diffraction (XRD) to confirm its characteristic properties. The surface area and pore volume of the resulting ACs decreased with increasing temperature. The samples obtained at 650°C of treatment have the maximum BET-specific surface area of 940 $m^2 g^{-1}$.

Keywords: Activated carbon; Chemical activation; Yerba mate.

Resumen

En este estudio, se prepararon carbones activados (AC) mediante activación química con $ZnCl_2$ de ramas de yerba mate (YM) en una proporción 1:1 masa de carbón vs masa de agente activador, realizándose la pirólisis a 550, 650 y 750 °C en una corriente de nitrógeno durante 60 y 120 minutos. Las muestras de AC se caracterizaron mediante diversas técnicas, como la isoterma de Brunauer-Emmett-Teller (BET), espectroscopía infrarroja por transformada de Fourier (FTIR), microscopía electrónica de barrido (SEM) y difracción de rayos X (XRD) para confirmar sus propiedades características. El área de superficie específica y el volumen de poros de los AC resultantes disminuyeron al aumentar la temperatura. Las muestras obtenidas a 650 °C mostraron superficies específicas BET máximas de 940 $m^2 g^{-1}$.

Palabras clave: Carbón activado; Activación química; yerba mate

Resumo

Neste estudo foram preparados carvões ativados (AC) por meio da ativação química com $ZnCl_2$ de ramos de erva-mate (YM) na proporção de 1:1 massa de carbono vs massa de agente ativador, com pirólise realizada a 550, 650 e 750° C em corrente de nitrogênio por 60 e 120 minutos. As amostras de AC foram caracterizadas por diversas técnicas, como isoterma de Brunauer-Emmett-Teller (BET), espectroscopia no infravermelho com transformada de Fourier (FTIR), microscopia eletrônica de varredura (SEM), difração de raios X (XRD) e para confirmar suas propriedades características. A área superficial específica e o volume dos poros dos AC resultantes diminuíram com o aumento da temperatura. As amostras obtidas a 650 °C apresentaram superfícies específicas BET máximas de 940 $m^2 g^{-1}$.

Palavras-chave: Carvão ativado; Ativação química; erva-mate

Introduction

Activated carbon (AC) is a porous solid with a large contact surface with the ability to capture and retain substances present in gaseous or liquid streams, such as in water treatment (1) and gas purification (2). There is a wide range of applications for ACs, including medicinal uses (3), gas storage, pollutant and odour removal, gas separations (4), catalysis (5), gas purification (4), metal extraction (6), water purification (7), chromatographic separation (8), chemical purification (9), heavy metal capture (10), fuel cells (11), spill clean-up, groundwater remediation (12), drinking water filtration (13), air purification (14), elimination of organic compounds, as well as other new processes that involve their use, such as in supercapacitors (11), electrodes or gas storage (15).

Various lignocellulosic residues, including agricultural by-products, have been explored as precursors for activated carbon due to their low cost and abundant availability. Studies have demonstrated that chemical activation with agents such as $ZnCl_2$ can lead to highly porous carbon structures, as observed in biomass sources like eucalyptus residue, coconut shells, sugarcane bagasse, and rice husk (16-20). The production of AC typically involves two steps (20). In the first stage, known as carbonization, the organic material undergoes thermal decomposition in an inert atmosphere, leading to the enrichment of carbon content and the partial removal of volatile compounds. This process initiates the formation of macro and mesopores as the biomass structure begins to break down. The remaining carbon skeleton, although porous, often lacks sufficient surface area and adsorption capacity for practical applications (21). These initial pore structures are significantly enhanced through chemical or physical methods during the subsequent activation process, depending on the activating agent used (22).

Activation can be achieved through two primary methods: physical activation and chemical activation, each with distinct mechanisms and outcomes. Physical activation involves using gases such as steam or carbon dioxide (CO_2) at high temperatures, typically ranging from 700 to 900°C. In this process, the carbonized material is exposed to a flow of steam or CO_2, which reacts with the carbon matrix, leading to the removal of surface carbon atoms through oxidation reactions. This controlled gasification gradually increases the material's porosity by enlarging existing pores and creating new ones, resulting in a highly porous structure with a wide distribution of micro and mesopores. Physical activation is often favoured for its ability to produce carbons with a well-defined pore structure. Still, it generally requires higher temperatures and longer processing times than chemical activation. (21, 23).

Chemical activation, on the other hand, is performed by impregnating the raw material with potent chemical agents such as zinc chloride ($ZnCl_2$), phosphoric acid (H_3PO_4), nitric acid (HNO_3), sulfuric acid (H_2SO_4), sodium carbonate (Na_2CO_3), sodium hydroxide (NaOH), or potassium hydroxide (KOH) (20-24). These chemicals act as dehydrating agents, breaking down the molecular structure of the raw material at lower temperatures, typically between 500 and 700°C, in an inert atmosphere such as nitrogen. The chemical agents facilitate the formation of a more extensive and uniform porous structure by preventing the excessive shrinkage of the material during pyrolysis, thus enhancing microporosity and surface area. After impregnation, the material undergoes carbonization, where the chemical agent either evaporates or remains incorporated in the structure, depending on the agent used. Chemical activation often results in higher yields and more developed microporosity than physical activation, making it a preferred method for producing activated carbon with high adsorption capacity and specific applications in gas purification, water treatment, and catalysis.

Chemical activation, as applied in this study with $ZnCl_2$, promotes the development of micropores by further decomposing the residual biomass and facilitating the rearrangement of carbon atoms (19). This increases the material's microporosity, surface area, and adsorption potential, which are critical for applications in environmental remediation and gas purification.

There is a lot of interest in using agro-industrial residues as AC precursors because they are cheap sources and available as by-products of other industries or processes (20). The production and industrialization of YM is carried out mainly in the provinces of Misiones and Corrientes of the Argentine Republic and reaches 277,000 annual tons of elaborated YM (25). According to estimates by the industrialists, there is a flow of dust and residual sticks of 3%, representing 8,000 tons of unused waste with potential for use as raw material in the production of AC.

YM sticks were used as AC precursors by means of chemical activation with $ZnCl_2$. The influence of the activation temperature and the activating agent's ratio on the obtained AC's characteristics were investigated, as in previous studies (26). The objective of this work is to assess how activation temperature and the ratio of activating agents affect the physicochemical properties of AC derived from yerba mate industrial waste, with the goal of optimizing its application in environmental remediation and adsorption processes.

Characterizing the AC's physicochemical properties is essential to determine its suitability for industrial and environmental applications, such as water treatment and gas purification. Key factors like specific surface area, porosity, and surface functional groups provide insight into its adsorption capacity and overall performance.

A higher specific surface area, measured by BET analysis, increases the number of adsorption sites, enhancing the AC's effectiveness in removing contaminants

like heavy metals and organic pollutants. Likewise, well-developed microporosity is crucial for capturing small molecules, making the material particularly suitable for gas purification and energy storage.

The functional groups, such as hydroxyl (OH) and carboxyl (COOH), identified through FTIR spectroscopy, further improve the AC's chemical interactions with contaminants, enhancing its adsorption properties. These analyses ensure the AC is optimized for high efficiency in various applications.

Materials and methods

Materials

YM sticks from an industrial plant were used, which were ground and sieved to a size between 0.45 and 1.60 mm. The proximal and component analysis of this material was performed as shown in **Table 1,** as in other publications (24). Deionized water and analytical-grade reagents were used for the experiments and determinations.

Table 1: Component analysis of YM sticks.

Component	(Dry base, %wt)[1]
Extractives [a]	14.09
Hemicelluloses	21.47
Celluloses	35.47
Lignin	20.96
[1] ethanol/methanol	

Preparation of activated carbon

The preparation of the activated carbon followed these steps: 1) the YM sticks were impregnated with a $ZnCl_2$ solution at 80 °C for 180 minutes by gentle agitation in a mass ratio of 1:1 carbon: $ZnCl_2$ (26). 2) the sample obtained was dried in an oven at 110°C for 24 h. 3) The impregnated sample was pyrolyzed in a fixed stainless-steel reactor 6 cm in diameter and 21 cm long at temperatures 550, 650, and 750°C for 1 and 2 hours with a flow of 1 ml.min^{-1} nitrogen at a heating rate of 10°C min^{-1}. 4) The carbonized samples were washed several times with distilled water at 90°C and finally with cold distilled water until the pH of the filtrate became neutral. 5) The washed samples were dried at 110°C for 24 hours to prepare the activated carbons. 6) The dried samples were ground to less than 74 microns. The nomenclature used for the AC samples is based on the activation temperature and the duration of the pyrolysis process.

The samples are designated as 'AC' followed by the activation temperature and the activation time. For example, 'AC650-1' refers to a sample activated at 650°C for 1 hour, while 'AC750-2' refers to a sample activated at 750°C for 2 hours. This systematic nomenclature allows for easy identification of the treatment conditions applied to each sample.

Characterization

Textural properties by nitrogen adsorption isotherm at 77 K

Surface characteristics such as pore structure and specific surface area of the resulting activated carbon materials were determined using physical nitrogen adsorption data obtained at 77K (equipment Micromeritics model ASAP 2000) (27). Before conducting the sorption experiments, the samples were exposed to a vacuum degasser at 180°C for 12 hours. Nitrogen adsorption/desorption data was used to determine BET-specific surface area, pore size distributions by the Quenched solid density functional theory method (QSDFT), and micropore volume by the Dubinin-Radushkevich method.

Surface Morphology by Scanning Electron Microscopy (SEM)

The morphological characteristics of the activated carbon were studied by scanning electron microscopy (SEM) (28). The apparatus used was a scanning electron microscope SEM-FEI-Quanta200, and two detectors were used: secondary electrons and X-rays.

X-ray diffraction analysis (XRD)

The X-ray diffraction (XRD) pattern of the carbonized material was obtained by applying the Bragg-Brentano technique (29), using a RIGAKU SmartLab SE diffractometer, operating at 40 kV and 50 mA, using Cu Kα radiation (k = 0.15406 nm), scanning 2θ with a range of 10–80°, scan speed 10°min^{-1}, and a step of 0.02°. The analysis of the crystalline phases was performed by comparing the diffractograms and the COD database (Crystallography Open Database).

Analysis of functional groups (FTIR)

The presence of functional groups on the activated carbon surface was investigated using a Fourier-transform infrared (28) spectrophotometer (equipment SHIMADZU model IRSpirit) in a frequency range of 600–4000 cm^{-1}. The samples for FTIR analysis were ground to a particle size smaller than 200 mesh (approximately 0.075 mm) to ensure homogeneity and accurate spectral readings.

Results and discussion

Structural Parameters

Table 2: shows the structural parameters of the ACs. For the samples obtained, the specific surface area was found in the range of 810 to 940 $m^2 g^{-1}$, while the pore volume varied from 0.35 to 0.42 $cm^3 g^{-1}$. The results obtained improved compared to those obtained by other authors (26).

It is observed that they are characterized by a microporous structure (VμP, **Table 2**). The contribution of the micropores was between 85 and 92% of its volume (%VμP, **Table 2**). This is seen by the shape of the nitrogen adsorption and desorption isotherms at 77K, which are type 1 isotherms (22) with minimal external surface area, as shown in **Figure 1,** and the pore volume distribution curves plotted in **Figure 2**.

The pore volume distribution curves show the peaks indicating the presence of micropores between 0.61 and 0.98 nm for the one-hour treatment (**Figure 2a**) and between 0.57 and 1 nm for the two-hour treatment (**Figure 2b**).

The reported results indicated that the YM bars gave a higher specific surface area than previous studies under similar activation conditions (26).

Table 2: Comparison of specific surface areas, micropore volume, and total pore volume

Sample	SBET (m^2g^{-1})	VμP1 (cm^3g^{-1})	VTP(0,98)2 (cm^3g^{-1})	$\%V_{\mu P}$ [3]
AC550-1	920	0.36	0.42	85.71
AC550-2	810	0.30	0.35	85.71
AC650-1	940	0.35	0.40	87.50
AC650-2	940	0.37	0.41	90.24
AC750-1	630	0.24	0.26	92.31
AC750-2	540	0.20	0.23	85.71

[1]Obtained by the Dubinin-Radushkevich method
[2]Obtained with Gurvich's Rule at $p/p^0 = 0.98$
[3]Obtained $(V_{\mu P}/V_{TP(0.98)})*100$

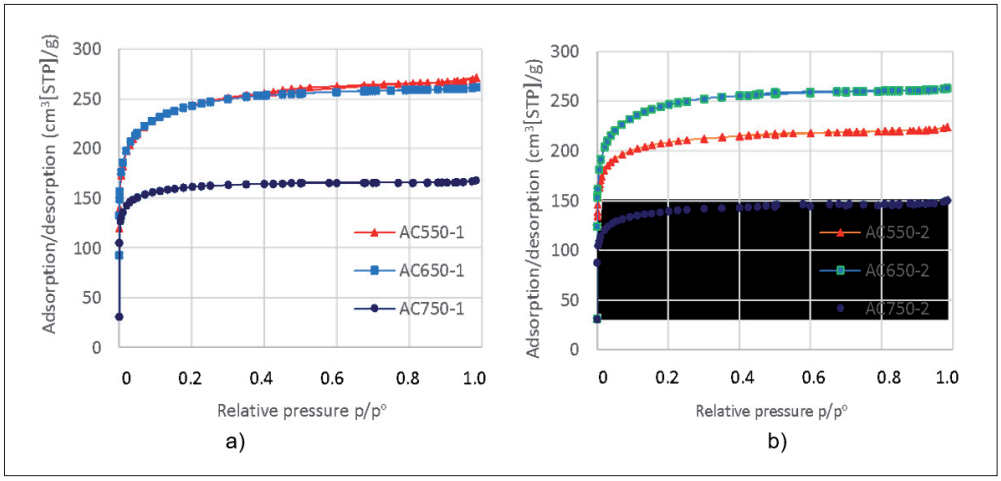

Figure 1: Nitrogen adsorption/desorption isotherms at 77 K for the AC obtained with 1 hour (a) and 2 hours (b) of pyrolysis.

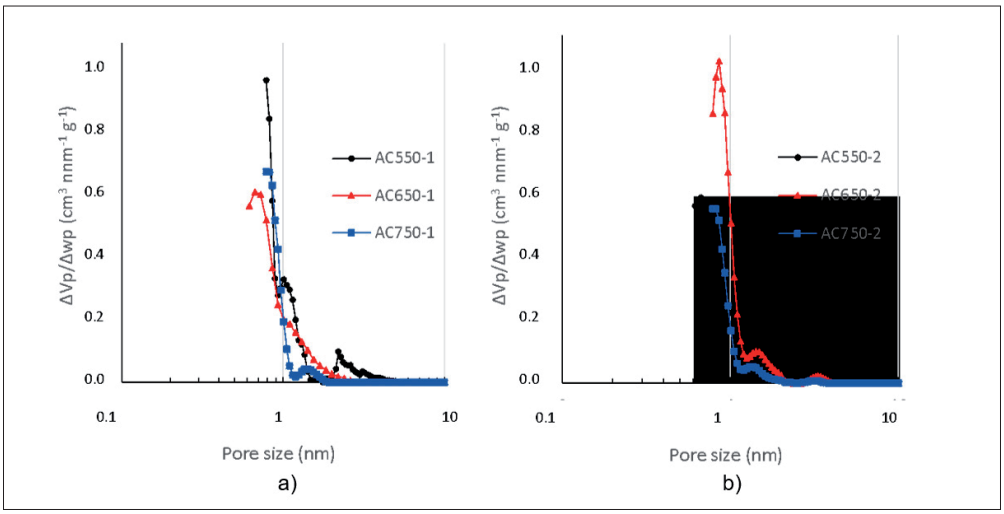

Figure 2: Pore size distribution curves for the AC obtained.

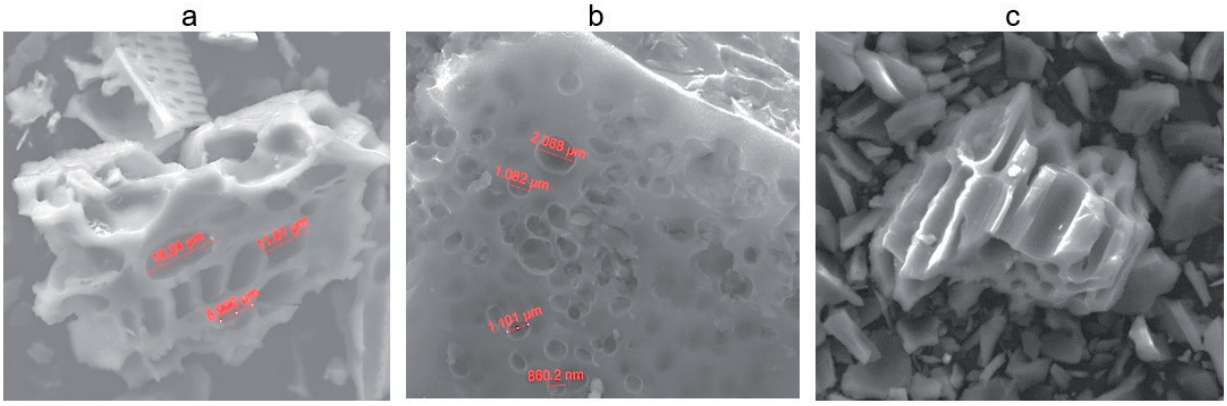

Figure 3: SEM of AC550-2 (a) AC650-2 (b) and AC750-2 (c)

The differences in microporosity between samples activated at different temperatures can be attributed to the degradation kinetics of organic matter, where higher temperatures favour the formation of smaller pores, as noted in the work by Benmahdi et al.

Surface Morphology by Scanning Electron Microscopy (SEM)

The surface structure of CA particles was analysed by SEM in the images shown in **Figure 3.** The external surface has cracks, crevices, and pores of various sizes in large holes. Likewise, the surface is heterogeneous, uneven, and rough, with many cavities, which can promote the diffusion and adsorption of molecules in the internal space of the particles.

It can be concluded from SEM images taken during the experiences carried out at carbonization temperatures between 550 and 750 ºC that a porous structure was formed because most of the organic volatiles were released, leaving the surface of the activated carbon with pores, in agreement with previous works (19,28).

X-ray diffraction analysis (XRD)

Figure 4 shows the XRD spectra of AC650-2. The broad blurred peaks at 2θ=15°–30° indicate that the carbon has mainly an amorphous structure. Peaks denoting zincite crystalline formations are observed primarily at a temperature of 650 °C. Although similar structures were observed across all treatments, they were more pronounced under these conditions. The low and broad diffraction peaks (2θ =40°–50°) can be related to the α axis of the graphite structure, which may indicate that the tested materials contain several graphite planes (30).

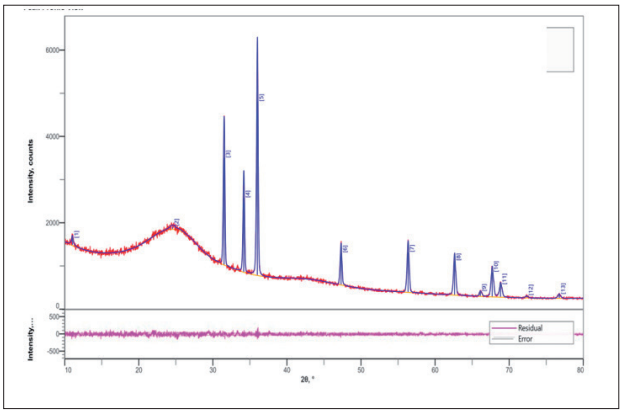

Figure 4: XRD spectra of AC650-2.

The XRD results indicate that the samples obtained exhibit crystalline phases, specifically zincite, which can be attributed to the activation treatment with $ZnCl_2$. The presence of these crystalline structures suggests that the chemical activation process promotes the formation of zinc-based phases, which are more pronounced at this temperature. This indicates that the activation conditions, particularly the use of $ZnCl_2$, play a critical role in facilitating the development of these crystalline phases.

Analysis of functional groups (FTIR)

Figure 5 presents the FTIR spectrum, highlighting characteristic bands between 1600 and 1024 cm^{-1} and at 850 cm^{-1}, typical of lignocellulosic materials and their derivatives. The band at 3325 cm^{-1} indicates the presence of –OH groups associated with alcohols and chemisorbed water. Additionally, the CA sample shows a reduction in the intensity of the C=C bonds found in lignin (1570 cm^{-1}), corresponding to the vibrations of aromatic rings. While similar patterns were observed in other treatments, this specific treatment was chosen due to its higher specific surface area, making it more suitable for adsorption applications. These findings are consistent with those reported in the literature (28), and the identified functional groups, such as hydroxyl and carbonyl, reflect the expected chemical changes during the pyrolysis of lignocellulosic residues.

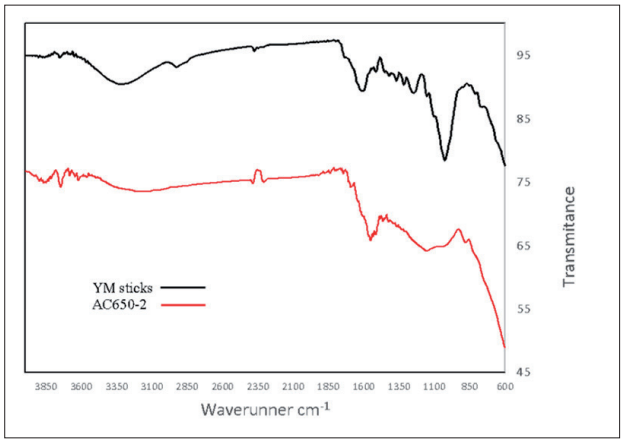

Figure 5: FTIR spectrum for the AC650-2 sample and its comparison with the YM sticks without processing.

Conclusions

In this study, ACs were successfully produced from yerba mate sticks through chemical activation with $ZnCl_2$, using a 1:1 mass ratio of activating agent to carbon. The activation process was carried out at temperatures ranging from 550 to 750°C, with activation times of 1 and 2 hours. The results indicate that AC samples activated for 1 hour at 650°C achieved the highest specific surface area, reaching 940 $m^2\ g^{-1}$. This high surface area is a critical property that enhances the adsorption capacity of the material, making it suitable for applications such as water treatment and gas purification.

FTIR spectroscopy confirmed the presence of key functional groups, such as hydroxyl (OH) and carbonyl (C=O), which are characteristic of lignocellulosic residues and were altered during the pyrolysis process. These groups play a vital role in the activated carbon's chemical reactivity and adsorption properties, facilitating the capture of contaminants in both liquid and gas phases. Additionally, the XRD analysis revealed the presence of crystalline phases, including zincite, especially at 650°C, which directly result from the $ZnCl_2$ activation process.

SEM analysis demonstrated that the AC produced has a highly porous structure with a wide range of pore sizes, which is crucial for its efficiency in adsorption processes. The well-developed microporosity, combined with the mesopores and macropores, ensures the material's versatility in adsorbing molecules of various sizes.

Although similar structural behaviours were observed across the different activation treatments, the 650°C sample was selected as the most promising due to its superior surface area and optimized pore structure. Furthermore, the grinding of samples to below 200 mesh (0.075 mm) for FTIR analysis ensured homogeneity and accurate characterization of the functional groups.

The findings of this study suggest that yerba mate sticks, an abundant agro-industrial residue, are a cost-effective and sustainable raw material for producing high-quality activated carbon. The material obtained through chemical activation with $ZnCl_2$ demonstrates excellent potential for industrial applications, offering a competitive alternative to conventional sources of activated carbon.

Acknowledgments

Thanks to the National Institute of Yerba Mate (INYM) for financing this research.

Thanks to Patricia Griselda Scipioni, M.S., for allowing the use of the facilities of the Organic Chemistry Laboratory of the FCEQyN and all the laboratory materials.

References

1. **Dubey, P., Shrivastav, V., Maheshwari, P. H., & Sundriyal, S.;** *Recent advances in biomass-derived activated carbon electrodes for hybrid electrochemical capacitor applications: Challenges and opportunities,* Carbon, 170; 1-29, 2020.
2. **Ma, F., Ding, S., Ren, H., & Liu, Y.;** *Sakura-based activated carbon preparation and its performance in supercapacitor applications,* RSC Advances, 9(5); 2474-2483, 2019.
3. **Tsivadze, A. Y., Gur'yanov, V. V., & Petukhova, G. A.;** *Preparation of spherical activated carbon from furfural, its properties and prospective applications in medicine and the national economy,* Protection of Metals and Physical Chemistry of Surfaces, 47; 612-620, 2011.
4. **Esteves, I. A., Lopes, M. S., Nunes, P. M., & Mota, J. P.;** *Adsorption of natural gas and biogas components on activated carbon,* Separation, and Purification Technology, 62(2); 281-296, 2008.
5. **Lee, J., Kim, J., & Hyeon, T.;** *Recent progress in synthesizing porous carbon materials,* Advanced Materials, **18(16); 2073-2094, 2006.**
6. **Li, Z., Chang, X., Zou, X., Zhu, X., Nie, R., Hu, Z., & Li, R.;** *Chemically-modified activated carbon with ethylenediamine for selective solid-phase extraction and preconcentration of metal ions,* Analytica Chimica Acta, 632(2); 272-277, 2009.
7. **Reza, M. S., Yun, C. S., Afroze, S., Radenahmad, N., Bakar, M. S. A., Saidur, R., & Azad, A. K.;** *Preparation of activated carbon from biomass and its applications in water and gas purification: A review,* Arab Journal of Basic and Applied Sciences, 27(1); 208-238, 2020.
8. **Postnov, V. N., Rodinkov, O. V., Moskvin, L. N., Novikov, A. G., Bugaichenko, A. S., & Krokhina, O. A.;** *From carbon nanostructures to high-performance sorbents for chromatographic separation and preconcentration,* Russian Chemical Reviews, 85(2); 115, 2016.
9. **Monser, L., Amor, M. B., & Ksibi, M.;** *Purification of wet phosphoric acid using modified activated carbon,* Chemical Engineering, and Processing: Process Intensification,

38(3); 267-271, 1999.

10. **Mariana, M., HPS, A. K., Mistar, E. M., Yahya, E. B., Alfatah, T., Danish, M., & Amayreh, M.**; *Recent advances in activated carbon modification techniques for enhanced heavy metal adsorption,* Journal of Water Process Engineering, 43; 102221, 2021.
11. **Dubey, P., Shrivastav, V., Maheshwari, P. H., & Sundriyal, S.**; *Recent advances in biomass-derived activated carbon electrodes for hybrid electrochemical capacitor applications: Challenges and opportunities,* Carbon, 170; 1-29, 2020.
12. **Hussain, O. A., Hathout, A. S., Abdel-Mobdy, Y. E., Rashed, M. M., Rahim, E. A., & Fouzy, A. S. M.**; *Preparation and characterization of activated carbon from agricultural wastes and their ability to remove chlorpyrifos from water,* Toxicology Reports, 10; 146-154, 2023.
13. **Heijman, S. G. J., & Hopman, R.**; *Activated carbon filtration in drinking water production: Model prediction and new concepts,* Colloids and Surfaces A: Physicochemical and Engineering Aspects, 151(1-2); 303-310, 1999.
14. **Gomez-Delgado, E., Nunell, G., Cukierman, A. L., & Bonelli, P.**; *Agro-industrial waste conversion into ultra microporous activated carbons for greenhouse gases adsorption-based processes,* Bioresource Technology Reports, 18; 101008, 2022.
15. **Musyoka, N. M., Wdowin, M., Rambau, K. M., Franus, W., Panek, R., Madej, J., & Czarna-Juszkiewicz, D.**; *Synthesis of activated carbon from high-carbon coal fly ash and its hydrogen storage application*, Renewable Energy, 155; 1264-1271, 2020.
16. **Han, Q., Wang, J., Goodman, B. A., Xie, J., & Liu, Z.**; *High adsorption of methylene blue by activated carbon prepared from phosphoric acid treated eucalyptus residue,* Powder Technology, 366; 239-248, 2020.
17. **Shamsuddin, M. S., Yusoff, N. R. N., & Sulaiman, M. A.**; *Synthesis and characterization of activated carbon produced from kenaf core fibre using H3PO4 activation,* Procedia Chemistry, 19; 558-565, 2016.
18. **Tay, T., Ucar, S., & Karagöz, S.**; *Preparation and characterization of activated carbon from waste biomass*, Journal of Hazardous Materials, 165(1-3); 481-485, 2009.
19. **Raut, E. R., Bedmohata, M. A., & Chaudhari, A. R.**; *Comparative study of preparation and characterization of activated carbon obtained from sugarcane bagasse and rice husk by using H3PO4 and ZnCl2,* Materials Today: Proceedings, 66; 1875-1884, 2022.
20. **Ukanwa, K. S., Patchigolla, K., Sakrabani, R., Anthony, E., & Mandavgane, S.**; *A review of chemicals to produce activated carbon from agricultural waste biomass*, Sustainability, 11; 6204, 2019.
21. **Yang, B., Liu, Y., Liang, Q., Chen, M., Ma, L., Li, L., Liu, Q., Tu, W., Lan, D., & Chen, Y.**; *Evaluation of activated carbon synthesized by one-stage and two-stage co-pyrolysis from sludge and coconut shell,* Ecotoxicology and Environmental Safety, 170; 722-731, 2019.
22. **Kwiatkowski, J. F.**; *Activated carbon: classifications, properties and applications,* **2012.**
23. **Zubrik, A., Matik, M., Hredzák, S., Lovás, M., Danková, Z., Kováčová, M., & Briančin, J.**; *Preparation of chemically activated carbon from waste biomass by single-stage and two-stage pyrolysis,* Journal of Cleaner Production, 143; 643-653, 2017.
24. **González-García, P.**; *Activated carbon from lignocellulosic precursors: A review of the synthesis methods, characterization techniques and applications,* Renewable and Sustainable Energy Reviews, 82; 1393-1414, 2018. https://inym.org.ar/descargar/publicaciones/estadisticas/2023.html
25. **Linhares, B., Weber, C. T., Foletto, E. L., Paz, D. S., Mazutti, M. A., & Collazzo, G. C.**; *Activated carbon prepared from yerba mate used as a novel adsorbent for removal of tannery dye from aqueous solution, Environmental Technology,* 34(16); 2401-2406, 2013.
26. **Foo, K. Y., & Hameed, B. H.**; *Mesoporous activated carbon from wood sawdust by K2CO3 activation using microwave heating, Bioresource Technology,* 111; 425-432, 2012.
27. **Saka, C.**; *BET, TG-DTG, FT-IR, SEM, iodine number analysis and preparation of activated carbon from a corn shell by chemical activation with ZnCl2,* Journal of Analytical and Applied Pyrolysis, 95; 21-24, 2012.
28. **Benmahdi, F., Oulmi, K., Khettaf, S., Kolli, M., Merdrignac-Conanec, O., & Mandin, P.**; *Synthesis and characterization of microporous granular activated carbon from Silver berry seeds using ZnCl2 activation*, Fullerenes, Nanotubes, and Carbon Nanostructures, 29(9); 657-669, 2021.
29. **Xu, J., Chen, L., Qu, H., Jiao, Y., Xie, J., & Xing, G.**; *Preparation and characterization of activated carbon from reedy grass leaves by chemical activation with H3PO4,* Applied Surface Science, 320; 674-680, 2014.